Eur. Phys. J. C 16, 361–366 (2000)
Digital Object Identifier (DOI) 10.1007/s100520000417

THE EUROPEAN PHYSICAL JOURNAL C

Supersymmetric hadronic bound state detection at e^+e^- colliders

M. Antonelli[1,a], N. Fabiano[2,b]

[1] Laboratori Nazionali di Frascati, INFN, Via E. Fermi 50, 00044 Frascati (Rome), Italy
[2] Physics Department of Perugia University and INFN, sezione di Perugia, Via A. Pascoli, 06123, Perugia, Italy

Received: 9 July 1999 / Revised version: 30 March 2000 /
Published online: 8 June 2000 – © Springer-Verlag 2000

Abstract. We review the possibility of formation for a bound state with a stop quark and its antiparticle. The detection of a signal from its decay has been investigated for the case of an e^+e^- collider.

1 Introduction

In the standard model it has been verified that bound states can be created for every quark but the top (see for instance [1–5] and references therein). The latter possibility is ruled out due to the high value of the top quark mass, which is responsible for its short lifetime. The natural next step would be to consider the possibility of bound state creation outside the standard model. In this case we focus our attention to the minimal supersymmetric extensions of the standard model (MSSM) [6], in particular to the resonant production [7,8] and detection of a bound state (supermeson) created from a stop and an anti-stop ("stoponium") at an e^+e^- collider.

2 Bound states

In this section we will review the creation of the bound state. For the SUSY case, our assumption will be that the creation of the bound state does not differ from the standard model (SM) case, as the relevant interaction is again driven by QCD and is regulated by the mass of the constituent (s)quarks.

A criterion for the formation of bound states is that [5] the formation of a hadron can occur only if the level splitting which depends upon the strength of the strong force between the (s)quarks and their relative distance [4] is larger than the natural width of the state. This means that, if

$$\Delta E_{2P-1P} \geq \Gamma, \tag{1}$$

where $\Delta E_{2P-1P} = E_{2P} - E_{1P}$ and Γ is the width of the would-be bound state, then the bound state exists.

For the case of a scalar bound state $\tilde{t}\bar{\tilde{t}}$, without reference to a particular supersymmetric model, we should consider the Coulombic two-body interaction

$$V(r) = -\frac{4}{3}\frac{\alpha_s}{r}, \tag{2}$$

with the two-loop expression for α_s [9]

$$\alpha_s(Q^2) = \frac{4\pi}{\beta_0 \log\left[Q^2/\Lambda^2_{\overline{\rm MS}}\right]} \times \left\{1 - \frac{2\beta_1}{\beta_0^2}\frac{\log\left[\log\left[Q^2/\Lambda^2_{\overline{\rm MS}}\right]\right]}{\log\left[Q^2/\Lambda^2_{\overline{\rm MS}}\right]}\right\}, \tag{3}$$

with $\beta_0 = 11 - (2/3)n_f$ and $\beta_1 = 51 - (19/3)n_f$. Due to the present limits on the stop mass [10,15] we could either assume that the stop is lighter than the top quark, that is $n_f = 5$, or heavier, i.e. $n_f = 6$. The expression for α_s, (3), has to be evaluated at a fixed scale $Q^2 = 1/r_B^2$, where r_B is the Bohr radius

$$r_B = \frac{3}{4\mu\alpha_s}, \tag{4}$$

and μ is the reduced mass of the system. It has been shown in [5,4] that in the case of high quark mass values, the predictions of the Coulombic potential evaluated at this scale do not differ from the other potential model predictions.

In Figs. 1 and 2 we show a plot of the energy splitting for the first two levels of the stoponium bound state with respect to the stop mass, for the LEP and the NLC case, respectively. As from (1), these figures have to be compared to the width of the stoponium. The width of the would-be stoponium, $\Gamma_{\tilde{t}\bar{\tilde{t}}}$, is twice the width of the single stop squark, as each should decay in a manner independent from the other. This value, of course, is not the total decay width of the stoponium bound state, as it includes only the single (s)quark decay modes and not the annihilation modes, which will be discussed in the next section. It represents the minimal energy level spread necessary for bound state formation which, if created, will in turn also have annihilation decay modes.

[a] e-mail: Mario.Antonelli@lnf.infn.it
[b] e-mail: Nicola.Fabiano@pg.infn.it

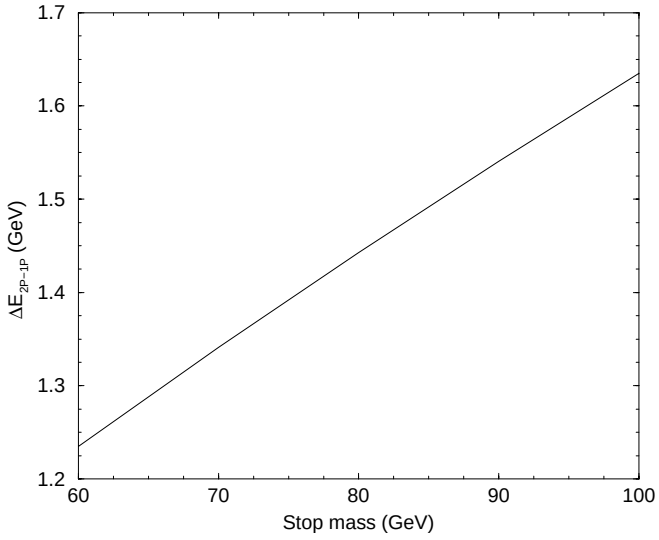

Fig. 1. ΔE_{2P-1P} as a function of the stop mass up to 100 GeV for the Coulombic model

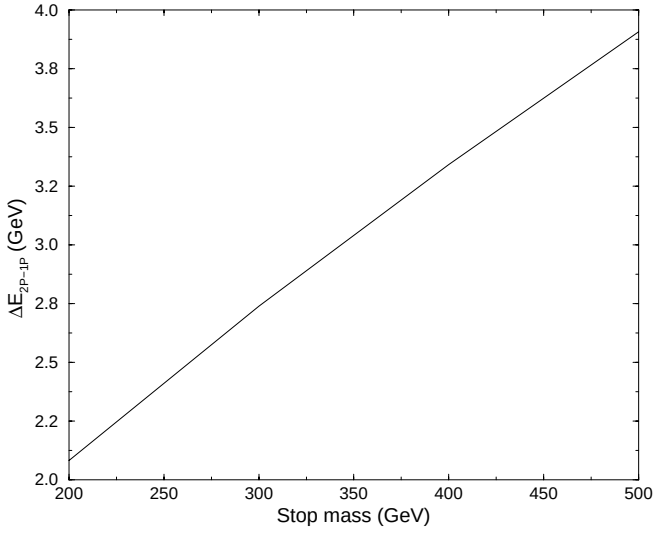

Fig. 2. ΔE_{2P-1P} as a function of the stop mass up to 500 GeV for the Coulombic model

There are several ways a stop could decay [16], depending on the assumptions made for the other superpartners. For very low values of the stop quark mass, the highest value of the width will not exceed a few keV, much smaller than the energy splitting of the first two levels. As the mass increases more decay modes enter and the width increases. In particular for the regime where $m_W + m_\chi + m_b < m_{\tilde{t}} < m_{\chi^+} + m_b$ the three-body decay $\tilde{t} \to bW\chi^0$ is kinematically allowed and is comparable to the flavor changing two-body decay $\tilde{t} \to c\chi$ [17]. Here χ refers to the lightest supersymmetric particle (LSP); χ^+ is the lightest chargino. Even in this case the widths do not exceed values in the keV range. In this scenario we see as before that the energy splitting is much larger than the decay width of the bound state; thus hadronization is possible.

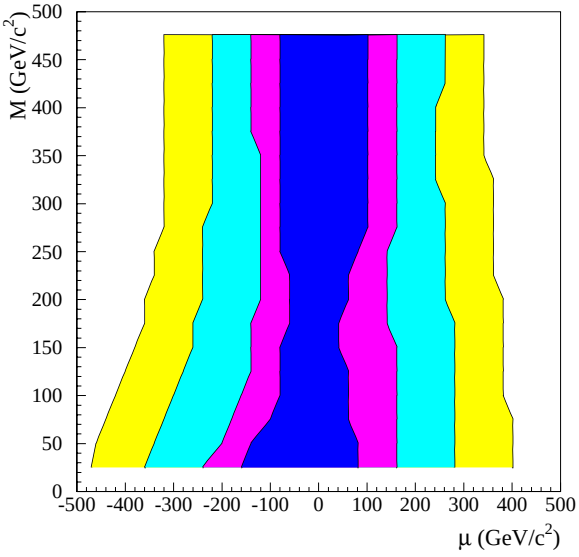

Fig. 3. Regions in the μ–M_2 plane where stoponium formation is forbidden; $\tan\beta = 1.5$. The different colors refer to various values of the stop mass: 250, 300, 400 and 500 GeV respectively, in increasing brightness

For even higher stop masses, the picture changes [18] as more two-body decays like $\tilde{t} \to b\chi^+$ and $\tilde{t} \to t\chi$ are available. For these values of the stop mass there are regions of parameter space where the decay widths, even if lowered by the one-loop corrections [18], could overtake the energy-level splitting, thus jeopardizing the formation of the supersymmetric bound state. For instance, in the region where $|\mu|$ is smaller than the stop mass the decay width can be larger than ΔE_{2P-1P} depending on the value of M_2, spoiling hadronization for $m_{\tilde{t}}$ beyond this range (here μ is the Higgs–higgsino mass parameter, while M_2 is the wino mass parameter). On the contrary, for parameter values where $\mu \gg M_{\tilde{t}}$, the decay width of these modes are substantially lower. This would allow stoponium formation for stop mass values in the energy range of the future NLC collider. The region where $\mu \sim M_{\tilde{t}}$ is in a situation intermediate between the two described above.

A quantitative description of the stoponium formation can be seen in Figs. 3 and 4, where we show the regions of the μ–M_2 plane for two values of $\tan\beta$ in which stoponium cannot be formed, for different values of the stop mass.

Regarding the hadronization problem we see that there are many possibilities due to the vast parameter space. For stop mass values under about 100–200 GeV and $\tan\beta = 1.5$ there is a window of opportunity for stoponium formation regardless of the parameter values; beyond that range the stoponium formation would either be allowed or forbidden depending upon the choice of the parameters.

It is interesting to study whether the points in the μ–M_2 plane where the bound state can be formed are still allowed by the several constraints that SUSY experimental searches have imposed. The LEP experiments [13] have published constraints in the μ–M_2 plane by using chargino and neutralino searches. However, the experimental limits are derived under the assumption that the trilinear

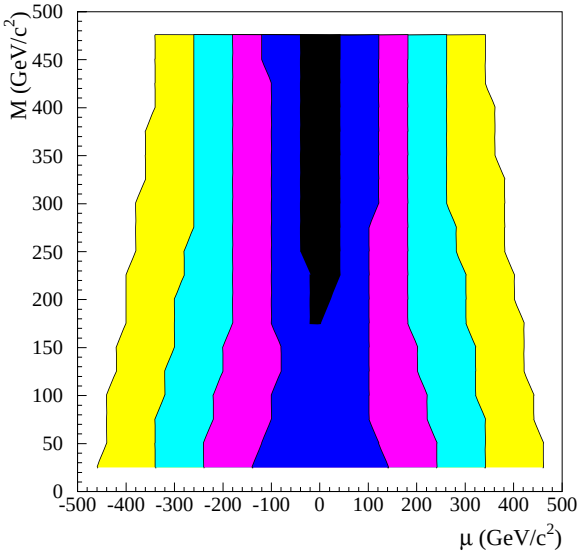

Fig. 4. Regions in the μ–M_2 plane where stoponium formation is forbidden; $\tan\beta = 40$. The different colors refer to various values of the stop mass: 100, 200, 300, 400 and 500 GeV respectively, in increasing brightness

coupling in the sfermion sector, A_f, is zero. This is a restrictive case for the stop sector, and experimental limits with a non-zero A_f have not yet been derived. Another potential constraint derives from the searches for Higgs bosons in the MSSM. The latest LEP results [14] show that the experimental lower limit on the Higgs mass overlaps the theoretical upper bound in the $\tan\beta$ range ~ 1–2. Moreover, these results are obtained without a scan on the MSSM parameters and in the MSSM space there are small regions with a vanishing $B(h \to b\bar{b})$. Therefore, also this constraint could be invalidated. Nevertheless the small $\tan\beta$ region is disfavored. Indirect searches provide restrictions on the possible form of new physics. In recent years powerful tests of the standard model have been performed, and restrictions for the MSSM parameters can be derived (see for instance [11,12]).

3 Cross section and decay width

The next natural step would be to see whether the stoponium could be detected at an e^+e^- collider with LEP or future NLC characteristics. For this purpose we shall calculate its cross section and decay modes; basing our predictions on [19], and updating the results therein.

We should look for the production and decay of the P wave state, since we are interested in the search of the bound state at a e^+e^- collider, thus conserving quantum numbers.

We use the Breit–Wigner formula to evaluate the total cross section [10]:

$$\sigma = \frac{3\pi}{M^2}\frac{\Gamma_e\Gamma_{\rm tot}}{(E-M)^2+\Gamma_{\rm tot}^2/4}, \tag{5}$$

where M is the mass of the resonance, E is the center-of-mass energy, $\Gamma_{\rm tot}$ is the total width, and Γ_e is the decay width to electrons.

The first decay we will investigate is the leptonic one, which is given by the Van Royen–Weisskopf formula [20]

$$\Gamma(2P \to e^+e^-) = 24\alpha^2\tilde{Q}^2\frac{|R'(0)|^2}{M^4}. \tag{6}$$

$R'(0)$ is the derivative of the radial wavefunction calculated at the origin, M the mass of the bound state, α the QED constant and $\tilde{Q}$ is

$$\left[Q^2 + \frac{1}{(M^2-M_Z^2)^2+M_Z^2\Gamma_Z^2}\left(\frac{M^4v_{\tilde{t}}^2(a_e^2+v_e^2)}{16\cos^4\theta_{\rm W}\sin^4\theta_{\rm W}} - \frac{QM^2v_ev_{\tilde{t}}(M^2-M_Z^2)}{2\cos^2\theta_{\rm W}\sin^2\theta_{\rm W}}\right)\right], \tag{7}$$

where $\sin^2\theta_{\rm W} = 0.213$, $v_e = (2\sin^2\theta_{\rm W} - 1/2)$, $a_e = -1/2$, M_Z and Γ_Z are respectively the mass and the width of the Z. The Z coupling to $\tilde{t}$–$\bar{\tilde{t}}$ is proportional to $v_{\tilde{t}} = 2(1/2\cos\theta_{\tilde{t}} - Q\sin^2\theta_{\rm W})$, $\theta_{\tilde{t}}$ being the mixing angle between $\tilde{t}_{\rm L}$ and $\tilde{t}_{\rm R}$. The interference of the γ and Z exchange contributions leads to a characteristic minimum of $\Gamma(2P \to e^+e^-)$ at $v_{\tilde{t}} \sim 0$. At $\theta_{\tilde{t}} = 0$, $\Gamma(2P \to e^+e^-)$ is maximal.

For this case and the following cases, we shall make use of the radial wavefunctions of the Coulombic model, as presented in Sect. 1. These are, for the $1S$ state

$$R_{1S}(r) = \left(\frac{2}{r_{\rm B}}\right)^{3/2}\exp\left(-\frac{r}{r_{\rm B}}\right), \tag{8}$$

and for the $2P$ state

$$R_{2P}(r) = \frac{1}{\sqrt{3}}\left(\frac{1}{2r_{\rm B}}\right)^{3/2}\frac{r}{r_{\rm B}}\exp\left(-\frac{r}{2r_{\rm B}}\right). \tag{9}$$

$r_{\rm B}$ is the Bohr radius defined in (4).

For the hadronic width decay we have the following expression:

$$\Gamma(2P \to 3g) = \frac{64}{9}\alpha_{\rm s}^3\frac{|R'(0)|^2}{M^4}\log(m_{\tilde{t}}r_{\rm B}), \tag{10}$$

where the Bohr radius acts as an infrared cutoff [19].

The $2P$ state could also decay into a $1S$ state and emit a photon. The decay width in this case is given by

$$\Gamma(2P \to 1S+\gamma) = \frac{4}{9}\alpha Q^2(\Delta E_{2P-1S})^3D_{2,1}, \tag{11}$$

where ΔE_{2P-1S} is the energy of the emitted photon, and $D_{2,1} = \langle 2P|r|1S\rangle$ is the dipole moment [21]. In Figs. 5 and 6 we present the decay widths of the $2P$ state into hadrons and into a $1S$ state plus a photon as a function of the stop mass, as predicted by the Coulombic model. In this case the behavior of the hadronic decay width with respect to the stop mass is $\Gamma(2P \to 3g) \sim m\alpha_{\rm s}^8$, while the radiative decay width goes like $\Gamma(2P \to 1S+\gamma) \sim m^2\alpha_{\rm s}^5$. In the

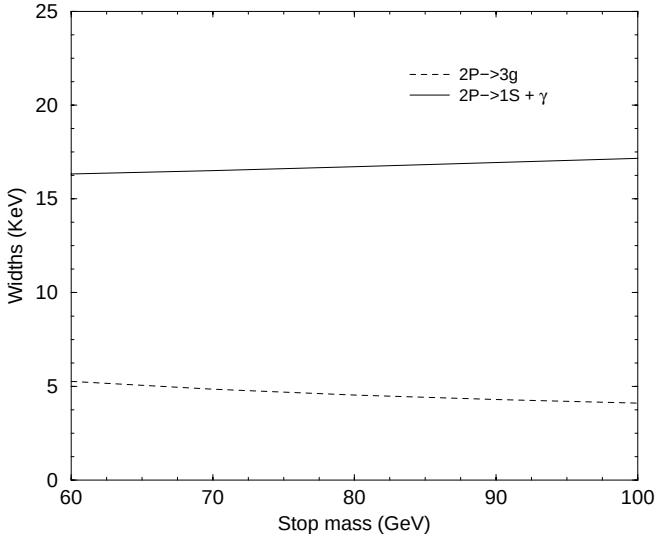

Fig. 5. Decay widths for the 2P state with respect to the stop mass for the Coulombic model. The dashed line represents the decay into hadrons, the continuous line the decay into the $1S$ state and an emitted photon

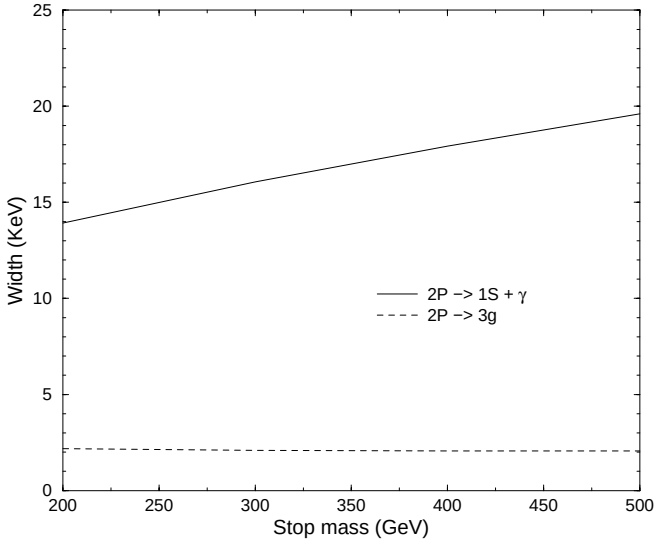

Fig. 6. Like Fig. 5, for a mass range of up to 500 GeV, for NLC

former case the linear growth with m is suppressed by the high power of α_s, resulting in an essentially constant width for the stop mass range of our interest. The $3g$ width will eventually grow faster for stop mass values larger than about 1 TeV. The behavior of the $2P \to 1S + \gamma$ decay is more straightforward, since its width grows faster with m and contains a lower power of α_s. It is also apparent that among the two, the $2P \to 1S + \gamma$ decay width dominates for increasing values of the stop mass, as clearly seen in Fig. 5 and particularly in Fig. 6. It is possible to notice also a small threshold effect due to the inclusion of the top flavor. Notice that annihilation decay modes through SUSY particle exchange can play an important role at high stop masses [7], making even more restrictive the former bound.

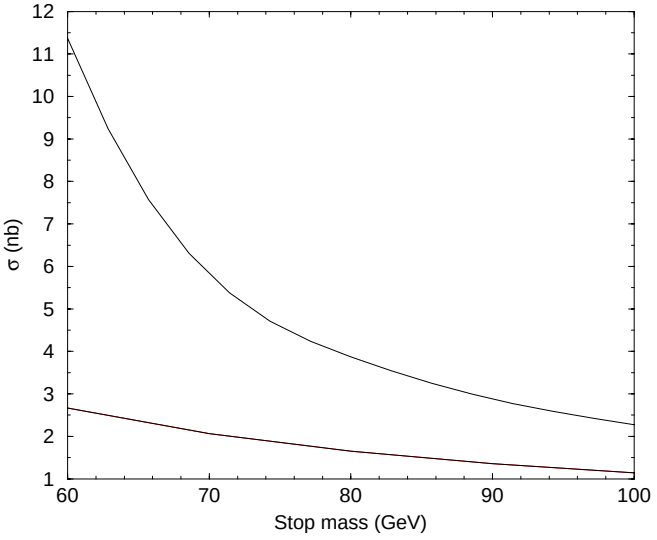

Fig. 7. Peak cross-section range as a function of the stop mass, for the LEP case, at Born level

We must point out that this behavior of decay widths of the stop bound state is given by the particular Coulombic potential model used in the computation. The results obtained however do not lose validity because, as has been shown in [2,4,5], this Coulombic model does not differ significantly from other more popular potential models when the mass of the constituent (s)quarks gets larger. This fact can be intuitively understood by considering the Bohr radius of the bound state, which decreases like $1/m$: therefore the constituent (s)quarks "feel" the Coulombic part of the potential more and more, this becoming dominant with respect to other components of the potential, like for instance the linear confining term that is added in the description of mesons containing lighter quarks.

For a stop lighter than all other SUSY particles but the neutralino, the analyzed annihilation modes are the dominant widths [16] so far. In this case the total width is minimal and the peak cross section is maximal.

Figure 7 shows the range of the peak cross section from minimal to maximal coupling of the $\tilde{t}$ to the Z obtained from (5) as function of the stop mass for a 200 GeV center-of-mass energy (LEP2).

While the peak cross section is in the nb range, the resonance is practically undetectable at the present collider because its width is much smaller than the typical beam energy spread (of the order of 200 MeV at LEP2 [10]). The effect of a growth of the total width due to the opening of other decay channels does not change the result, as the net effect will be a decrease of the peak cross section. This is clearly illustrated in Fig. 8 where the Breit–Wigner formula (5) is folded with the typical energy spread of the beam of 200 MeV. We should notice that even in the most favorable case of maximal coupling to the Z boson there is not a clear improvement of the signal.

The possibility of stoponium production with radiative returns has also been considered and the results for the cross-section range are illustrated in Fig. 9. We see that

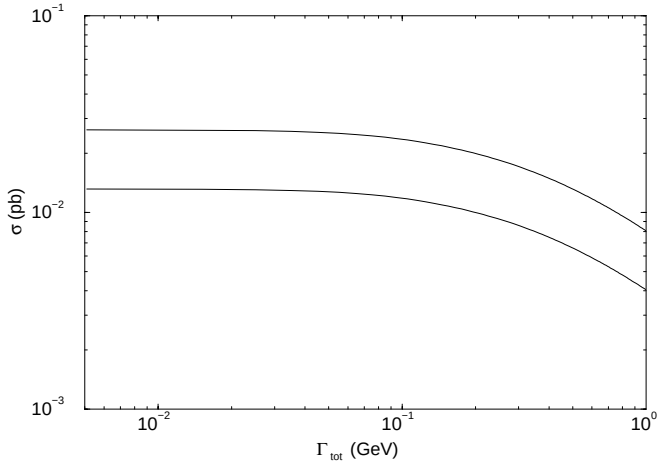

Fig. 8. Total cross-section range folded with a beam energy spread of 200 MeV as a function of the total width of the stop, at Born level. The plot has been obtained for a stop mass of 100 GeV

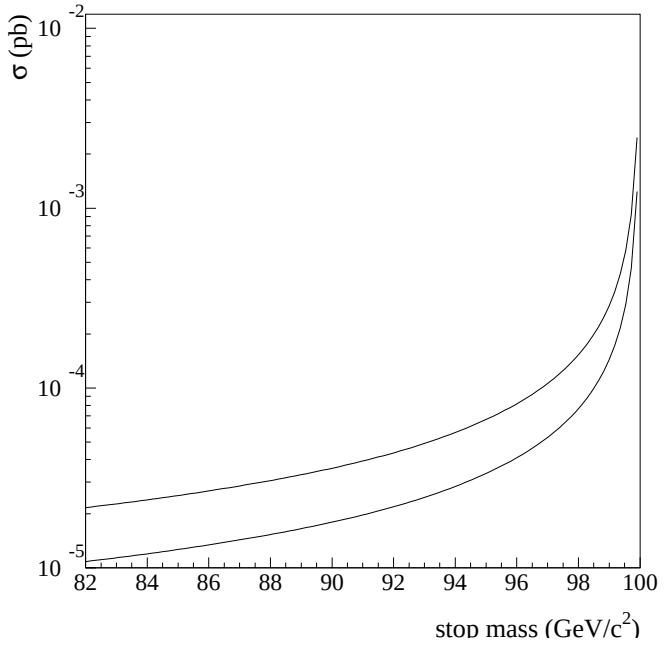

Fig. 9. Radiative return production cross-section range as a function of the stop mass, for the LEP case

the cross section is quite small, and in this manner there is no possibility of seeing any signal.

With the increase of the center-of-mass energy (NLC case) the scenario changes: as more decay channels appear there are regions in the parameter space where stoponium cannot be formed. The net result for the signal detection does not change, as could clearly be seen in Figs. 10 and 11 where we show the effective total cross-section range and the radiative return cross-section range for a center-of-mass energy of 500 GeV. Again, as seen in the LEP case, the factor given by (7) is not sufficient to significantly improve the signal.

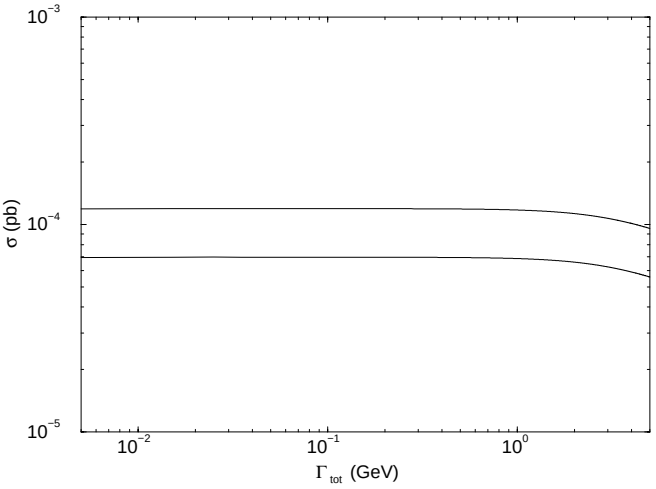

Fig. 10. Like Fig. 8, for a beam energy spread of 6 GeV (NLC) [22]. The plot has been obtained for a stop mass of 200 GeV

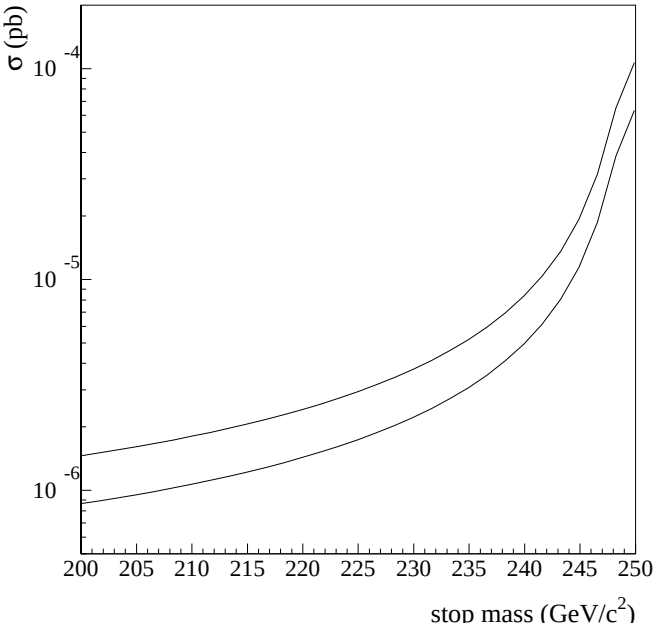

Fig. 11. Radiative return production cross-section range as a function of the stop mass, for the NLC case

4 Conclusions

We have shown that because of the high energy binding and the narrow decay width the formation of a $\tilde{t}\bar{\tilde{t}}$ P wave bound state is possible in certain regions of the parameter space, and in particular for a light stop. However, our result shows that this supersymmetric bound state cannot be detected at the present and even at the future e^+e^- collider. The latter fact proves also that it gives a negligible contribution to the $\tilde{t}\bar{\tilde{t}}$ production cross section.

Acknowledgements. We would like to thank V. Khoze for careful reading of the manuscript. One of us (N.F.) wishes to thank A. Masiero for useful discussion.

References

1. V.S. Fadin, V.A. Khoze, JETP Lett. **46**, 525 (1987); Yad. Fiz. **48**, 487 (1988); I. Bigi, V.S. Fadin, V.A. Khoze, Nucl. Phys B **377**, 461 (1992)
2. G. Pancheri, J.P. Revol, C. Rubbia, Phys. Lett. B **277**, 518 (1992)
3. J.H. Kühn, E. Mirkes, Phys. Lett. B **296**, 425 (1992); Phys. Rev. D **48**, 179 (1993)
4. N. Fabiano, Eur. Phys. J. C **2**, 345 (1998)
5. N. Fabiano, A. Grau, G. Pancheri, Phys. Rev. D **50**, 3173 (1994); Nuovo Cimento A, **107**, 2789 (1994)
6. For a review see: Supersymmetry and supergravity, edited by M. Jacob
7. M. Drees, M. Nojiri, Phys. Rev. D **49**, 4595 (1994)
8. W. Mödritsch, Phys. Lett. B **349**, 525 (1995)
9. W.A. Bardeen, A.J. Buras, D.W. Duke, T. Muta, Phys. Rev. D **18**, 3998 (1978); W.J. Marciano, Phys. Rev. D **29**, 580 (1984)
10. Review of Particle Properties, EuroPhys. J. C **3**, 1 (1998); http://pdg.lbl.gov/
11. L. Giusti, A. Romanino, A. Strumia, Nucl. Phys. B 550 (1999); G. Altarelli, R. Barbieri, F. Caravaglios, Int. J. Mod. Phys. A **13**, 103 (1998)
12. M. Ciuchini, G. Degrassi, P. Gambino, G.F. Giudice, Nucl. Phys. B **534**, 3 (1998); For a review, see M. Misiak, S. Pokorski, J. Rosiek, in Heavy Flavours II, edited by A.J. Buras, M. Lindner (World Scientific, Singapore 1998) hep-ph/9703442; S. Khalil, A. Masiero, Q. Shafi, Phys. Rev. D **56**, 5754 (1997)
13. OPAL Collaboration, Search for chargino and neutralino production at $s^{1/2} = 189\,\mathrm{GeV}$ at LEP, CERN-EP/99-123
14. Talks to the LEPC, 9 November 1999. See for instance: http://alephwww.cern.ch/ALPUB/seminar/seminar.html and http://www.cern.ch/Opal/
15. ALEPH Collaboration, Search for sleptons and squarks in e^+e^- collisions at 189 GeV, Phys. Lett. B **469**, 303 (1999); Search for light top squarks in $p\bar{p}$ collisions at $s^{1/2} = 1.8\,\mathrm{TeV}$, Phys. Rev. Lett. **76**, 2222 (1996)
16. K. Hikasa, M. Kobayashi, Phys. Rev. D **36**, 724 (1987); A. Bartl et al., Phys. Lett. B **384**, 151 (1996); Z. Phys. C **73**, 469 (1997)
17. W. Porod, T. Wöhrmann, Phys. Rev. D **55**, 2907 (1997)
18. A. Djouadi, W. Hollik, C. Jünger, Phys. Rev. D **55**, 6975 (1997); see also references therein
19. C. Nappi, Phys. Rev. D **25**, 84 (1982)
20. R. Van Royen, V. Weisskopf, Nuovo Cimento A **50**, 617 (1967)
21. J. Kühn, P.M. Zerwas, Phys. Rev. **167**, 321 (1988)
22. Conceptual design of a 500 GeV e^+e^- linear collider with integrated X-ray laser facility, edited by R. Brinkmann, G. Materlik, J. Rossbach, A. Wagner, Vol. 1 (1997); Ron Settles, private communication; Marcello Piccolo, private communication